Two Faces of Chondroitin Sulfate Proteoglycan in Spinal Cord Repair: A Role in Microglia/Macrophage Activation

Asya Rolls[1☯], Ravid Shechter[1☯], Anat London[1], Yifat Segev[1], Jasmin Jacob-Hirsch[2], Ninette Amariglio[2], Gidon Rechavi[2], Michal Schwartz[1*]

1 Department of Neurobiology, The Weizmann Institute of Science, Rehovot, Israel, **2** Cancer Research Center, Sheba Medical Center and Sackler School of Medicine Tel-Aviv University, Ramat Aviv, Israel

Funding: This study was supported, in part, by an NRSAD award and partially supported by an Israel Amyotrophic Lateral Sclerosis Research Association (IsrALS) grant given to MS, and by research grants from Mr. and Mrs. Richard D. Siegal. The funders had no role in study design, data collection and analysis, decision to publish, or preparation of the manuscript.

Competing Interests: The authors declare that they have no competing interests.

Academic Editor: Wolfgang Streit, University of Florida, United States of America

Citation: Rolls A, Shechter R, London A, Segev Y, Jacob-Hirsch J, et al. (2008) Two faces of chondroitin sulfate proteoglycan in spinal cord repair: A role in microglia/macrophage activation. PLoS Med 5(8): e171. doi:10.1371/journal.pmed.0050171

Received: August 22, 2007
Accepted: July 7, 2008
Published: August 19, 2008

Abbreviations: BDA, biotinylated dextran amine; BDNF, brain-derived neurotrophic factor; BMS, Basso mouse scale; BrdU, 5-bromo-deoxyuridine; ChABC, chondroitinase ABC; CNS, central nervous system; CSPG, chondroitin sulfate proteoglycan; GFAP, glial fibrillary acid protein; GFP, green fluorescent protein; IGF-1, insulin-like growth factor 1; IP, intraperitoneal(ly); IRS-1, insulin receptor substrate 1; LPS, lipopolysaccharide; MMP, matrix metalloproteinase; PDL, poly-D-lysine; SD, standard deviation; TNF-α, tumor necrosis factor alpha

* To whom correspondence should be addressed. E-mail: michal.schwartz@weizmann.ac.il

☯ These authors contributed equally to this work.

ABSTRACT

Background

Chondroitin sulfate proteoglycan (CSPG) is a major component of the glial scar. It is considered to be a major obstacle for central nervous system (CNS) recovery after injury, especially in light of its well-known activity in limiting axonal growth. Therefore, its degradation has become a key therapeutic goal in the field of CNS regeneration. Yet, the abundant de novo synthesis of CSPG in response to CNS injury is puzzling. This apparent dichotomy led us to hypothesize that CSPG plays a beneficial role in the repair process, which might have been previously overlooked because of nonoptimal regulation of its levels. This hypothesis is tested in the present study.

Methods and Findings

We inflicted spinal cord injury in adult mice and examined the effects of CSPG on the recovery process. We used xyloside to inhibit CSPG formation at different time points after the injury and analyzed the phenotype acquired by the microglia/macrophages in the lesion site. To distinguish between the resident microglia and infiltrating monocytes, we used chimeric mice whose bone marrow-derived myeloid cells expressed GFP. We found that CSPG plays a key role during the acute recovery stage after spinal cord injury in mice. Inhibition of CSPG synthesis immediately after injury impaired functional motor recovery and increased tissue loss. Using the chimeric mice we found that the immediate inhibition of CSPG production caused a dramatic effect on the spatial organization of the infiltrating myeloid cells around the lesion site, decreased insulin-like growth factor 1 (IGF-1) production by microglia/macrophages, and increased tumor necrosis factor alpha (TNF-α) levels. In contrast, delayed inhibition, allowing CSPG synthesis during the first 2 d following injury, with subsequent inhibition, improved recovery. Using in vitro studies, we showed that CSPG directly activated microglia/macrophages via the CD44 receptor and modulated neurotrophic factor secretion by these cells.

Conclusions

Our results show that CSPG plays a pivotal role in the repair of injured spinal cord and in the recovery of motor function during the acute phase after the injury; CSPG spatially and temporally controls activity of infiltrating blood-borne monocytes and resident microglia. The distinction made in this study between the beneficial role of CSPG during the acute stage and its deleterious effect at later stages emphasizes the need to retain the endogenous potential of this molecule in repair by controlling its levels at different stages of post-injury repair.

The Editors' Summary of this article follows the references.

Introduction

The poor recovery of the central nervous system (CNS) following an injury is generally attributed to the accumulation of compounds that mediate self-perpetuating degeneration, the presence of growth inhibitors [1,2], formation of the glial scar [3,4], and a malfunction of the immune response mediated mostly by microglia/macrophages [5–8]. The extracellular matrix molecule chondroitin sulfate proteoglycan (CSPG) is a major constituent of the glial scar [1,9–11], and it is intensively secreted following CNS injury. Its effect on recovery in the CNS has gained a negative reputation that derives mainly from studies in which it was shown to impede axonal regeneration [9,10]. This perception prompted attempts to overcome this obstacle to recovery, especially by the use of chondroitinase ABC (ChABC), a CSPG-degrading enzyme [1,12,13], aimed at elimination of CSPG from the injury site. Moreover, the observed spatial and temporal association between CSPG deposition and the local immune response was thought to support the negative roles of both in recovery from CNS injury [3].

Accumulated data suggest, however, that a tightly regulated and timely immune response is needed for recovery [14–17]. It is now apparent that the phenotype of microglia/macrophages is not uniform [15,18–24], and that in response to different stimuli these cells can acquire either destructive [25–31] or a beneficial phenotype [32–34]. These latter observations, together with the fact that the postinjury increase in CSPG is not restricted to the CNS but is a general phenomenon associated with the healing of wounds [35], led us to postulate that the intense de novo synthesis of CSPG following injury might have a role in the repair process by regulating the local immune response, and that its overall negative reputation might reflect nonoptimal regulation of its production and/or degradation.

Methods

Animals

Two mouse strains were used in the experiments, inbred adult wild-type C57Bl/6J mice (supplied by the Animal Breeding Center of The Weizmann Institute of Science) and CX3CR1$^{GFP/+}$ mice (a generous gift of Stefan Jung at the Weizmann Institute). The CX3CR1$^{GFP/+}$ mice are heterozygotic mice with green fluorescent protein (GFP) inserted in the CX3CR1 locus in one allele, while a normal allele enables the continued expression of CX3CR1 [36]. In these mice, all myeloid cells express GFP. Chimeric mice were generated as described below, by replacing the bone marrow of wild-type mice with bone marrow derived from the CX3CR1$^{GFP/+}$ mice. Newborn C57Bl/6J mice were used for the extraction of microglia, used in the in vitro studies. All animals were handled according to the regulations formulated by the Institutional Animal Care and Use Committee (IACUC).

Summary of Animal Groups

The experiments described in Figure 1 included five C57Bl/6J and four chimeric mice subjected to spinal cord injury. Figure 2 shows data from 13 C57Bl/6J and eight chimeric mice subjected to spinal cord injury and treated with either PBS or xyloside, and analyzed by immunohistochemistry. In Figure 3, for the dose–response to xyloside, 21 animals were subjected to spinal cord injury and were divided into four experimental groups. The functional recovery assessments shown in Figure 3 and Figure 4 included 42 mice subjected to spinal cord injury. These mice were divided into five groups and were assessed for motor recovery. At the end point, the mice were killed and lesion size was determined by immunohistochemistry (Figure 4H and 4I). An additional eight mice were used for biotinylated dextran amine (BDA) analysis (Figure 4F and 4G). CSPG levels were determined in an independent experiment (Figure 4J and 4K) that included 16 mice, subjected to spinal cord injury, divided into four groups and analyzed 14 d later. For Western blotting, nine mice divided into three groups were included and were analyzed 7 d after the injury. In Figure 5, IGF-1 assessment was examined 14 d after spinal cord injury, by immunohistochemistry and ELISA, and included 14 and 16 mice, respectively. For the assessment of GFP+ infiltrating cells (Figure 5D), 14 d after the injury, a total of eight chimeric mice were subjected to spinal cord injury and divided into two groups. Results in Figures 6 and 7 do not include in vivo experiments. In Figure 8, 33 mice were subjected to spinal cord injury and divided into two groups (PBS control and CSPG-DS treatment) and were followed for motor functional recovery. For histology, 12 mice were also subjected to spinal cord injury and assessed 14 d later by immunohistochemistry. BDA analysis was performed on another group of eight animals, subjected to injury and either left untreated or treated with CSPG-DS. For all ELISA results reported within the text, analysis was performed 14 d after spinal cord injury, and four mice were used in each group.

Spinal Cord Injury and Assessment of Functional Recovery

The spinal cords of anesthetized mice were exposed by laminectomy at T12, and a force of 200 kdyn was placed for 1 s on the cord by using the Infinite Horizon spinal impactor (Precision Systems, Lexington, Kentucky), a device shown to inflict a well-calibrated injury of the spinal cord. The animals were maintained on twice daily bladder expression. Functional recovery from spinal cord contusion in mice was determined by hind limb locomotor performance. Recovery was scored by the Basso mouse scale (BMS), an open-field locomotor rating scale [37], that was developed specifically for mice, with scores ranging from 0 (complete paralysis) to 9 (normal mobility). Blind scoring ensured that observers were not aware of the treatment received by each group (7–20 mice per group; mice were excluded in cases of peritoneal infection, wounds in the hind limbs, and tail and foot autophagia). Twice a week, locomotor activities of mice in an open field were monitored by placing the mouse for 4 min at the center of a circular enclosure (90 cm in diameter, 7 cm wall height) made of molded plastic with a smooth, nonslip floor.

ELISA

Wild-type C57Bl/6J mice were killed and their spinal cords were removed 14 d after spinal cord injury. A section of 1 mm^2 from the lesion area or from a noninjured area 1 cm distally to the injury site (repeated with six mice per group) was excised. The excised tissue was homogenized in PBS. Similarly, in an independent experiment, we excised the lesion area in PBS or xyloside-treated (0.8 mg/mouse for 6 d, immediately, 2 or 7 d after the injury) mice (four mice per group). Two freeze-thaw cycles were performed to break the

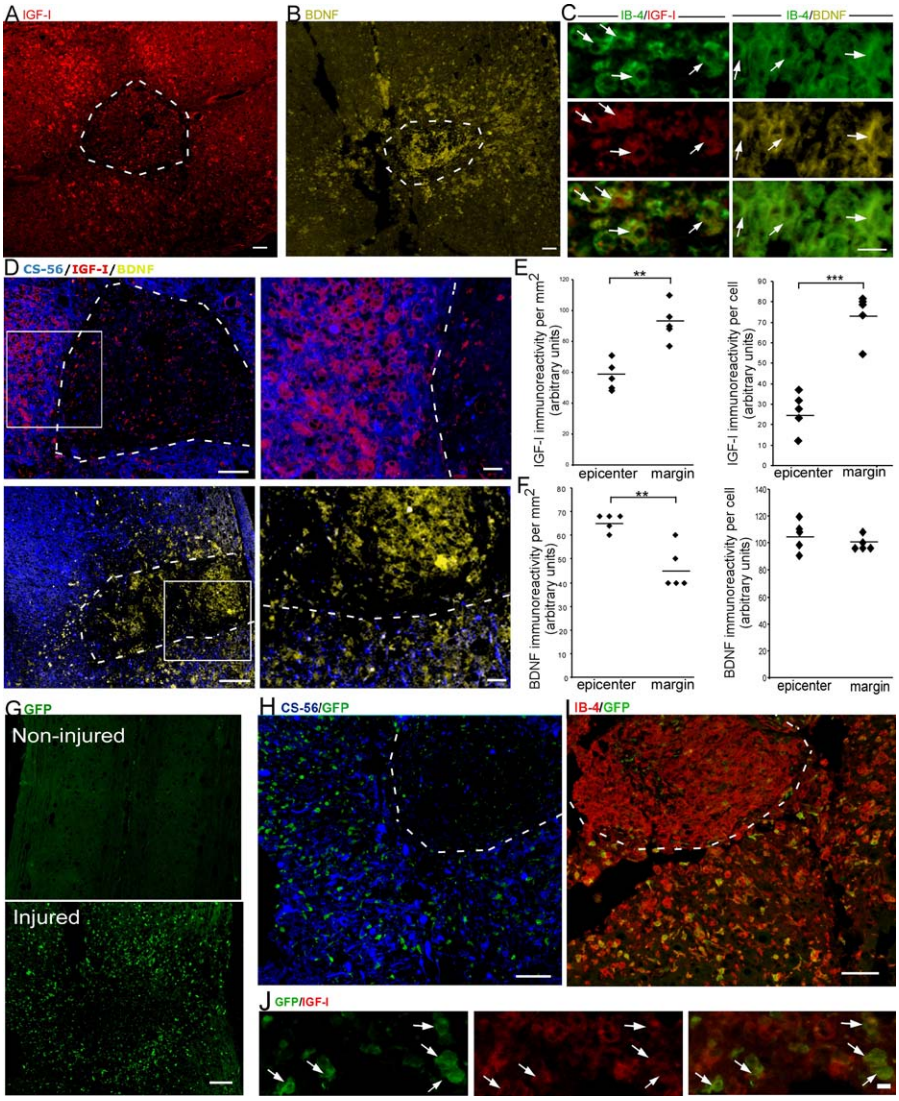

Figure 1. Microglia and Blood-borne Monocytes Associated with CSPG Found in the Lesion Site Express High Levels of IGF-1

Paraffin-embedded spinal cord sections were prepared from the lesion site 14 d after injury.

(A and B) Sections were immunolabeled for IGF-1 (A) or BDNF (B) (scale bar 500 μm).

(C) Sections were labeled with IB-4 (green), to identify microglia/macrophages and IGF-1 (red; left panels) or BDNF (yellow; right panels) (scale bars, 10 μm; arrows indicate double-labeled cells).

(D) Labeling by CS-56 (blue), a marker of CSPG and IGF-1 (red, upper panels) colocalized at the margins of the lesion site. BDNF expression (yellow, lower panels) is not specifically colocalized with CS-56 immunoreactivity (blue, all panels; scale bar, 100 μm). High-power images of the boxed area in the left panels are shown on the right (scale bar, 20 μm).

(E and F) Quantitative analysis of IGF-1 (E) and BDNF (F) immunoreactivity, at the epicenter and the margins of the lesion calibrated to either intensity per square millimeter. Total intensity in the examined region was normalized to the size of the area (left graphs, arbitrary units, Student *t*-test, [E] $t = -5.03$, df = 8; $p = 0.001$; [F] $t = 4.55$, df = 8, $p = 0.002$) or intensity per cell (total intensity in the examined region normalized to the number of IB-4 labeled cells; right graphs, arbitrary units, Student *t*-test: [E] $t = -7.4$, df = 8, $p = 0.0001$; [F] $t = 0.97$, df = 8, $p = 0.36$). *$p < 0.05$; **$p < 0.01$; ***$p < 0.001$.

(G) Sections from GFP-chimeric mice labeled for GFP (blood-derived macrophages; green) in non-injured and injured mice (scale bar, 100 μm).

(H and I) Lesion site in chimeric injured mice, labeled for CS-56 (blue) (H) and GFP (green) or IB-4 (red) (I) and GFP (green; scale bars 10 μm).

(J) High magnification of cells from the marginal area of the lesion, indicating that both GFP-positive (green) and GFP-negative cells express IGF-1 (red; scale bar, 20 μm). Arrows indicate blood-derived macrophages (GFP-positive) cells expressing IGF-1. In all panels, boundaries between the epicenter and the margins are marked by dashed line.

doi:10.1371/journal.pmed.0050171.g001

cell membranes, and the homogenates were centrifuged for 5 min at 5,000*g*, the total protein levels were determined by Bradford reagent, and equal amounts of protein in equal volumes were then assayed using ELISA (Quantikine Mouse IGF-1 or TNF-α Immunoassay, R&D Systems), according to the instructions of the manufacturer. Results are expressed by picograms of protein per milliliter of homogenate.

Chimeric Mice

C57BL/6J-CX3CR1$^{GFP/+}$ chimeric mice were generated by lethal whole body irradiation (950 rad, with shielding of the brain) of C57BL/6J mice followed by reconstitution with 4×10^6 bone marrow cells isolated from the CX3CR1$^{GFP/+}$ mice (harvested from the femora and tibiae, by flushing the bones with Dulbecco PBS under aseptic conditions, and then

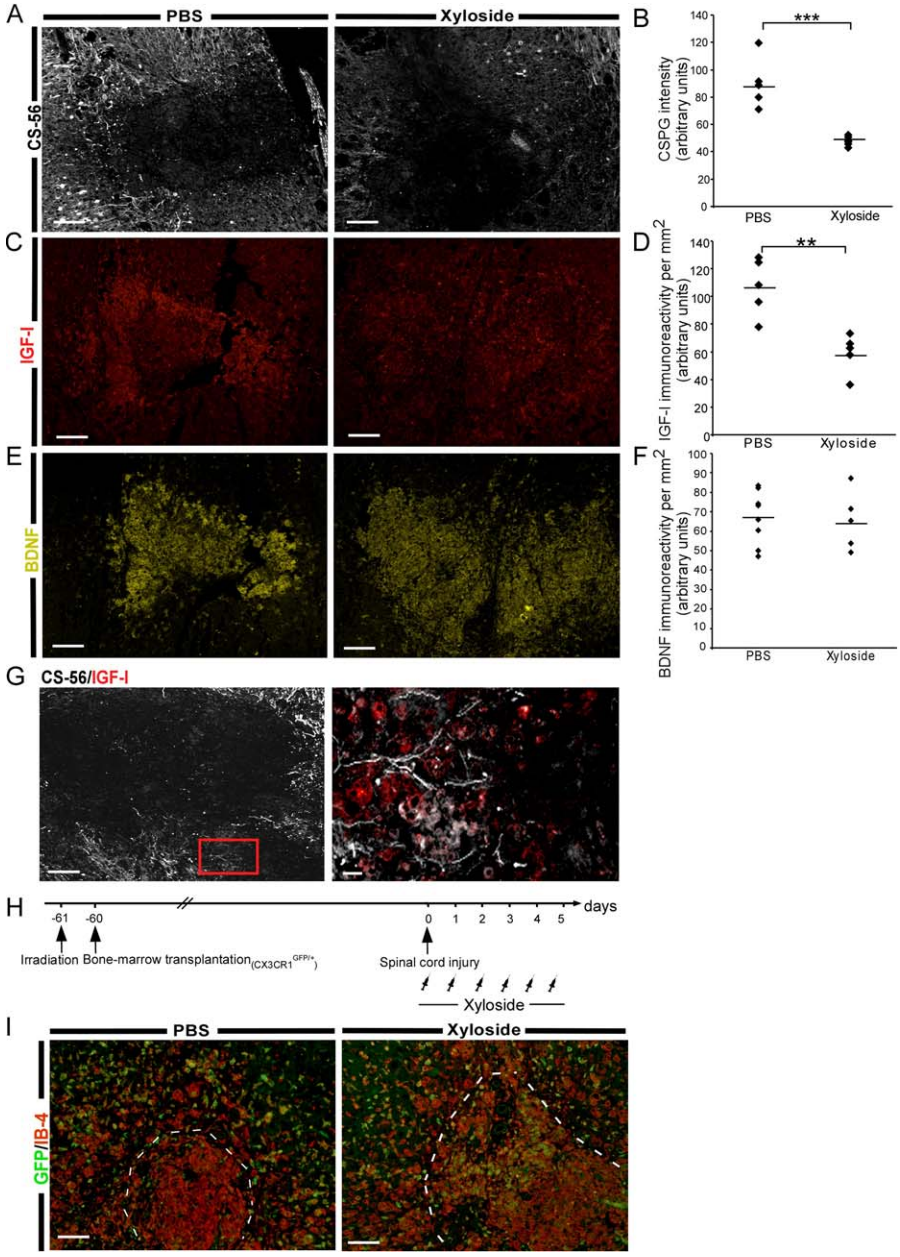

Figure 2. CSPG Modulates Microglia/Macrophage Activation and Spatial Localization in the Lesion Site

After spinal cord injury, mice were injected IP with xyloside (1.2 mg/mouse/d, for 6 d), a pharmacological inhibitor of CSPG synthesis.
(A) CS-56 staining of spinal cord sections for the presence of CSPG (scale bar, 250 μm).
(B) Quantitative analysis of CSPG intensity in the diameter of 1 mm around the epicenter (arbitrary units; Student *t*-test, $t = 5.61$, df = 9, $p = 0.0003$).
(C) Staining for IGF-1 (red; scale bar, 250 μm).
(D) Quantitative analysis of IGF-1 immunoreactivity per square millimeter, at the site (arbitrary units; Student *t*-test, $t = 4.5$, df = 8, $p = 0.002$).
(E) Staining for BDNF (yellow; scale bar, 250 μm).
(F) Quantitative analysis of BDNF immunoreactivity at the site (arbitrary units; nonsignificant according to Student *t*-test, $t = 0.21$, df = 11, $p = 0.83$).
(G) Representative photomicrographs of CS-56-labeled spinal cord sections from mice treated with xyloside (scale bar, 250 μm). The boxed area in the left panel is magnified on the right and shows labeling for IGF-1 (red) and CS-56 (CSPG; white; scale bar, 20 μm).
(H) Scheme showing experimental time scale. Bone marrow chimeras were generated by reconstitution of irradiated C57BL/6J mice with $CX_3CR1^{GFP/+}$ bone marrow. After 2 mo, chimeric mice were subjected to spinal cord injury and injected IP with xyloside.
(I) Staining for GFP (green; blood-borne macrophages) and IB-4 (red; microglia/macrophages) at the injury site in control (left) and in xyloside-treated (right) animals (scale bar, 100 μm; ** $p < 0.01$; *** $p < 0.001$).
doi:10.1371/journal.pmed.0050171.g002

collected and washed by centrifugation for 10 min at 1,000 rpm at 4 °C), in which GFP is expressed under the promoter of the chemokine receptor, CX3CR1. In the chimeric mice formed following bone marrow reconstitution, the bone marrow-derived cells (blood-borne monocytes) originating from the $CX3CR1^{GFP/+}$ mice express GFP; however, the resident microglia are GFP-negative. This system thus allows the resident microglia and the infiltrating macrophages to be distinguished. The mice were grafted with bone marrow cells 2 mo before the spinal cord injury.

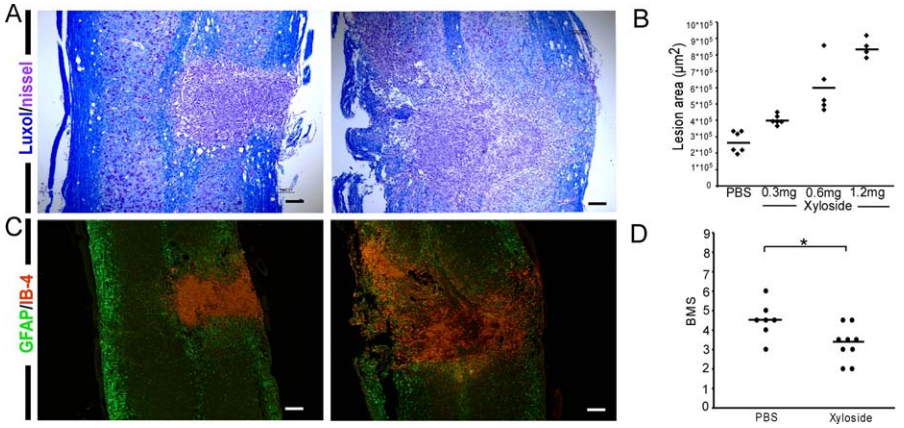

Figure 3. CSPG Plays a Key Role in Recovery from Spinal Cord Injury

(A) Staining for myelin by Luxol (blue) and to nuclei by Nissel (pink) (scale bar, 500 μm).

(B) Quantitative analysis of the size of the site of injury as a function of the xyloside dosages, determined by Luxol and Nissel staining (ANOVA, $F[3,17] = 37.5$, $p = 0.0001$, followed by Fisher test for differences between groups). Results were significant at the 5% level in all cases except for xyloside treatment (0.3 mg/d) compared to PBS, and for xyloside treatment at 0.3 mg/d compared to 0.6 mg/d.

(C) Immunohistochemistry of xyloside-treated spinal cords, using anti-GFAP (green) antibodies and IB-4 labeling (red) (scale bar, 250 μm).

(D) Mean locomotor score (BMS) of individual mice on day 36 after spinal cord injury with and without xyloside treatment (immediately after injury 0.8 mg/mouse/d; Student *t*-test, $t = 2.67$, $df = 14$, $p = 0.018$). * $p < 0.05$.

doi:10.1371/journal.pmed.0050171.g003

Xyloside Treatment

Xyloside (4-methylumbelliferyl-β-D-xylopyranoside; Sigma-Aldrich) was injected intraperitoneally (IP) every day starting either immediately after the injury, 2 d later, or 7 d after the injury. The mice were injected twice daily for 5 d. The mice were analyzed for functional recovery with the BMS, cytokine expression by ELISA, and CSPG expression by Western blotting (using wild-type C57Bl/6J mice) and histology (using wild-type and chimeric mice). For functional analysis, mice were examined up to 60 d after injury. For histological analysis mice were killed 14 d after the injury. Several dosages of xyloside, adapted from another experimental system [38], were tested in order to choose the lowest effective dose (0.8 mg/mouse). To exclude the possibility that the effects of xyloside result from a peripheral effect on the bone marrow or cell composition in the blood, rather than from the elimination of CSPG from the lesion site, we examined the effects of xyloside application on cellular blood composition, bone marrow cell populations, and bone marrow architecture (Figure S1). All the examined parameters were similar in the xyloside-treated and the control groups (three mice per group). Analysis was performed using standard procedures by a commercial service (Pathovet, Kefar Bilu, Israel).

CSPG-DS Administration

CSPG-DS (6-sulfated disaccharides; Sigma-Aldrich), were administered to mice by repeated intravenous injections (5 μg dissolved in PBS) on days 1, 4, 7, 10, and 13 after injury.

Anterograde BDA Labeling

Wild-type C57Bl/6J mice that were followed for functional recovery were anesthetized 60 d after the injury, and injected bilaterally using a stereotaxic frame, with the high-resolution anterograde tracer BDA (10,000 MW lysine-fixable biotin dextran amine; Molecular Probes, Eugene, OR; 1.2 μl of 10% wt/vol BDA solution in 0.01 M PB). BDA was injected into both motor cortices. A 30-gauge Hamilton needle was lowered through the cortex (1 mm) and four injections of 0.3 μl per site were administered within a perimeter defined coronally by bregma 1.7 mm to −0.7 mm, and sagittally 0.5–1.5 mm from the sagittal suture, bilaterally. Injections were performed over 3–5 min and the needle was slowly removed. The mice were killed and perfused 14 d after BDA injection. For histological assessment of the BDA tracing, spinal cords, and brains were dissected, and sections (30 μm) of the thoracic spinal cord comprising the lesion site were cut either horizontally (floating) or longitudinally, and stained for BDA by the use of either nickel-enhanced diaminobenzidine protocol [39], or fluorescently labeled Cy3-strepavidin (Jackson ImmunoResearch), as indicated in the relevant legends. Injection site and labeling are shown in Figure S2. To quantify anterogradely labeled fibers caudal to the lesion, we calculated the labeling caudal to the lesion site relative to the amount of BDA-labeled axons rostal to the lesion for each animal.

Immunohistochemistry

Mice subjected to spinal cord injury were killed 14 d later, their spinal cords were prepared for histology and analyzed as described before [40] (3–5 mice per group). The following antibodies were used: mouse anti-CS-56 (1:100; Sigma-Aldrich), chicken anti-BDNF (1:100; Promega), goat anti-IGF-1 (1:20; R&D Systems) rabbit anti-mouse glial fibrillary acid protein (GFAP 1:200; DakoCytomation), and rabbit anti-GFP (1:100; MBL). For microglial cell/macrophage labeling we used FITC-conjugated *Bandeiraea simplicifolia* isolectin B4 (IB-4; 1:50; Sigma-Aldrich) for 1 h in the secondary antibody solution. Secondary antibodies used were Cy3-conjugated donkey anti-goat antibody, Cy3-conjugated donkey anti-chicken antibody, and Cy2/Cy5 conjugated donkey anti-mouse antibody (1:200; all from Jackson ImmunoResearch). The slides were exposed to Hoechst stain (1:2000; Invitrogen Probes) for 1 min. The same antibodies were used for immunohistochemical analysis of the microglia cultured in vitro.

Myelin integrity was qualitatively examined on paraffin-embedded sections that were stained with Luxol fast blue for

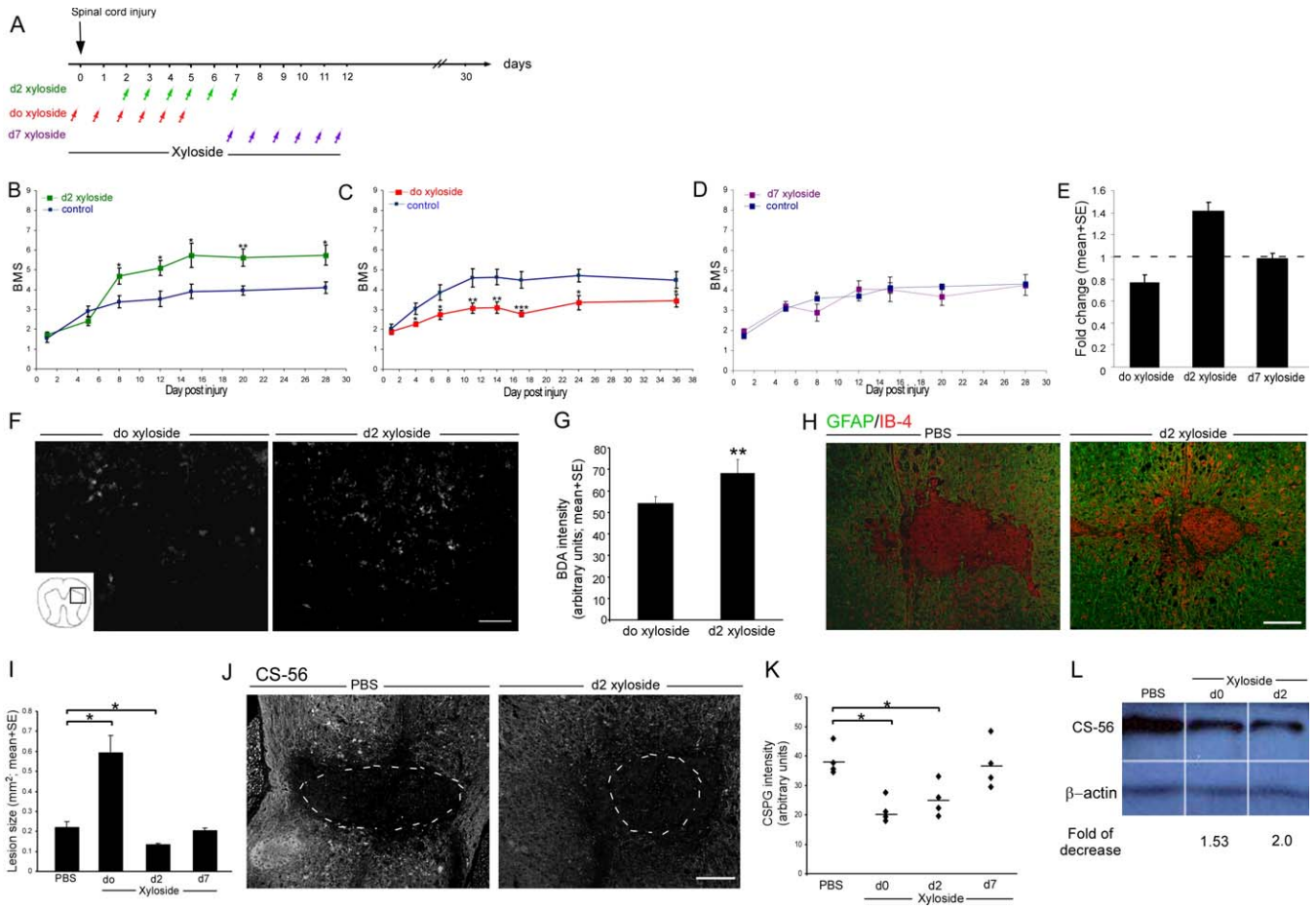

Figure 4. Restricting CSPG Secretion to the Acute Stage after Injury Improves Functional Recovery

(A) Schematic representation of the experimental time scale. Mice were subjected to contusive spinal cord injury and were treated with xyloside (0.8 mg/mouse/d for 6 d) at different time points after the injury. Locomotion was recorded, and is given by the mean locomotor scores (BMS) for each group.

(B) Xyloside application started 2 d after the injury (repeated measures ANOVA, F[1,15] = 7.426 [between groups], $p = 0.016$).

(C) Xyloside application started immediately after the injury (two factor repeated measures ANOVA, F[1,14] = 15.481 [between groups], $p = 0.0015$).

(D) Xyloside application started 7 d after the injury (repeated measures ANOVA, F[1,15] = 0.093 [between groups], $p = 0.764$).

(E) Fold change in functional recovery on day 30 after the injury between each treatment compared to their matched untreated control (ANOVA, F[2,27] = 16.64, $p = 0.0001$).

(F) BDA tracing of the corticospinal tract, caudal to the lesion site in a xyloside-treated mouse; photomicrographs show cornal sections excised from mice treated with xyloside on day 0 (left) or 2 (right) after the injury (scale bars, 250 μm). Insert shows the site from which the images were taken.

(G) Quantitative analysis of BDA labeling. To quantify labeled fibers caudal to the lesion, we calculated the labeling caudal to the lesion site relative to the amount of BDA rostal to the lesion for each animal (mean ± SD; Student *t*-test, $t = -3.99$, df = 6, $p = 0.007$).

(H) Immunohistochemistry of xyloside-treated spinal cords, using anti-GFAP (green) antibodies and IB-4 labeling (red; scale bars, 250 μm).

(I) Quantitative analysis of the size of the injury site as a function of the treatment, determined by Luxol and Nissel staining (ANOVA, F[3,26] = 43.03, $p = 0.0001$).

(J) CS-56 staining of spinal cord sections, excised from mice 14 d after the injury, for the presence of CSPG (scale bar, 250 μm). The dashed line demarcates the lesion site, defined based on GFAP labeling.

(K) Quantification of CSPG intensity (ANOVA, F[3,12] = 7.619, $p = 0.0041$).

(L) Western blot analysis of CSPG levels in the control group (PBS) and in the groups receiving xyloside treatment on day 0 or day 2 after the injury (excised 7 d after the injury). β-actin was used as a control for protein levels. Fold decrease in CSPG levels, relative to PBS control, are shown ($n = 3$ mice per group).

ANOVA in (I) and (K) followed by the Fisher test for differences among groups (significant at the 5% level). Asterisks (G, I, and K) denote statistically significant differences between the indicated groups, or compared to the relevant control: *$p < 0.05$; **$p < 0.01$.

doi:10.1371/journal.pmed.0050171.g004

myelin and Nissel for the nuclei and the thin cytoplasmic layer around them. With the aid of Image-Pro (Media Cybernetics) the results were analyzed by determination of the density or by measurement of the lesion area by an observer who was blinded to the treatment received by the mice. For tissue cultured cell phosphorylated ERK labeling, mouse anti phosphoERK (Santa Cruz) was used. For analysis, 500–1,000 cells were sampled for each marker.

Quantification

For microscopic analysis a Nikon florescent microscope was used (Nikon E800). Intensity of staining was calibrated using Image-Pro Plus software by an observer blind to the identity of the slides. To calibrate intensity of labeling, an average of sampled background areas was subtracted from the total intensity counted. To demonstrate intensity per square millimeter, the total intensity in the examined region

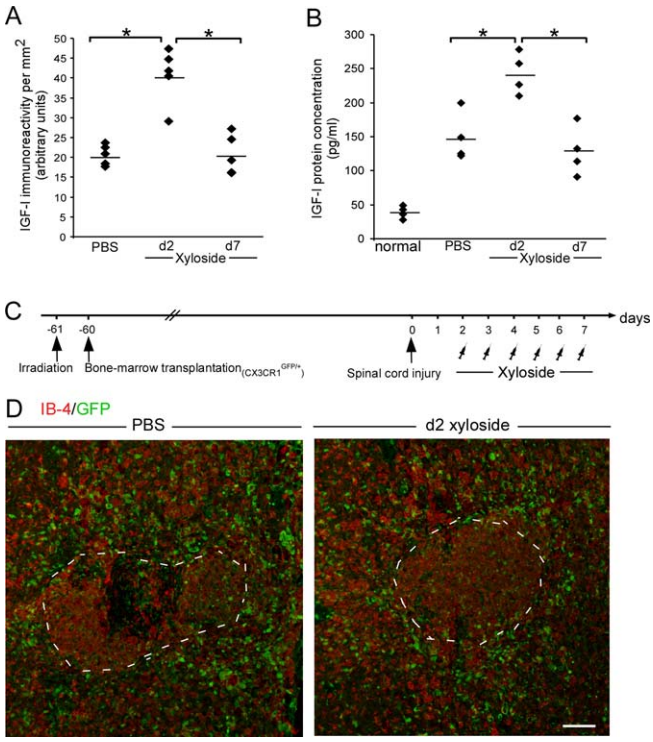

Figure 5. Delayed Inhibition of CSPG Synthesis Positively Modulates Activation and Spatial Localization of Microglia/Macrophages in the Lesion Site

Spinal cords were excised (14 d after the lesion) from animals that were subjected to spinal cord injury and treated with either PBS or with xyloside administered on day 2 or day 7 following the insult.

(A) Quantitative analysis of IGF-1 immunoreactivity per square millimeter at the site (ANOVA, $F[2,11] = 22.78$, $p = 0.0001$).

(B) Quantitative analysis of IGF-1 protein concentration determined by ELISA of spinal cord tissue (ANOVA, $F[3,12] = 32.138$, $p = 0.0001$).

(C) Experimental time scale. CX3CR1$^{GFP/+}$ > wild type bone marrow chimeras were generated by reconstitution of irradiated C57BL/6J mice with CX3CR1$^{GFP/+}$ bone marrow. Chimeric mice were subjected to spinal cord injury and injected IP with xyloside starting from day 2 after the injury.

(D) Staining for GFP (green; blood-borne macrophages) and IB-4 (red; microglia/macrophages) at the injury site in control (PBS) and in delayed (day 2) xyloside-treatment group (scale bar, 250 μm).

ANOVA followed by the Fisher test for differences between groups; significant differences at the 5% level are denoted by asterisks. All the groups in (B) were significantly different from uninjured control.

doi:10.1371/journal.pmed.0050171.g005

was normalized to the size of the area. To determine cell numbers, we counted the cells using manual tagging within the Image-Pro Plus software. To determine intensity per cell, total intensity in the examined region was normalized to the number of cells. For each assessment, four or five animals per group were examined, sections from three different depths were examined, and at least 1,000 cells per group were included. The margins and the lesion size were defined by the area demarcated by GFAP immunolabeling or Luxol/Nissel staining (the lesion was identified as the area that was not labeled for myelin by Luxol) and quantified by Image-Pro Plus software.

Western Blotting

Wild-type C57Bl/6J mice were killed 7 d after the spinal cord injury, and sections of the spinal cord (5 mm around the lesion site) were removed. The sections were shock-frozen in liquid nitrogen and homogenized in 150 mM NaCl, 1% NP-40, 0.5% sodium deoxycholate, 0.1% SDS, 50 mM Tris (pH 8.0) containing proteinase inhibitor cocktail (Sigma), 1 mM leupeptin, and 1 mM pepstatin. The homogenates were incubated for 1 h and centrifuged at 10,000*g* for 15 min. Bradford analysis was performed to determine protein concentrations, and similar levels of protein were subjected to 5% SDS-PAGE and detected using CS-56 antibody (Sigma) and anti-β-actin. The gels were calibrated using the NIH Image program, the intensity of each CS-56 band was calibrated relative to its β-actin levels, and the fold decrease compared to PBS treatment was determined (three mice were examined in each group).

Tissue Culture

To prepare cultures of microglia, a distinct group of neonatal (P0–P1) C57Bl/6J mice was used. The mice were killed and their brains were stripped of their meninges and minced with scissors under a dissecting microscope (Zeiss, Stemi DV4, Germany) in Leibovitz-15 medium (Biological Industries, Beit Ha-Emek, Israel). After trypsinization (0.5% trypsin, 10 min, in 5% CO_2 at 37 °C), the tissue was triturated. The cell suspension was washed in culture medium (DMEM supplemented with 10% fetal calf serum [Sigma-Aldrich], 1 mM l-glutamine, 1 mM sodium pyruvate, 100 U/ml penicillin, and 100 μg/ml streptomycin). The mixed brain glial cells were cultured in 5% CO_2 at 37 °C in 75-cm^2 Falcon tissue culture flasks (BD Biosciences) that had been coated with poly-d-lysine (PDL) (10 μg/ml; Sigma-Aldrich) in borate buffer (15.45 g boric acid [Merck] dissolved in 500 ml of sterile water [pH 8]) for 1 h, then rinsed thoroughly with sterile, glass-distilled water. The medium was changed after 24 h in culture, and every second day thereafter, for a total culture time of 10–14 d. Microglia were shaken off the primary mixed brain glial cell cultures (150 rpm, 6 h, 37 °C) with maximum yields between day 10 and 14, and seeded (10^5 cells/ml) on coverslips coated with PDL or CSPG (Sigma-Aldrich) for the indicated time periods. Cells were grown in culture medium for microglia (RPMI-1640 medium [Sigma-Aldrich] supplemented with 10% fetal calf serum, 1 mM l-glutamine, 1 mM sodium pyruvate, 50 μM β-mercaptoethanol, 100 U/ml penicillin, and 100 μg/ml streptomycin). Since CSPG was used in the present study as a matrix component rather than as a soluble compound, its effect was monitored as a function of time, rather than as a function of dose. Cell proliferation was visualized by staining with 5-bromo-deoxyuridine (BrdU, 2.5 μM; Sigma-Aldrich). Lipopolysaccharide (LPS; Sigma-Aldrich) was added to the culture medium after the cells were cultured on CSPG or treated with CSPG-DS. For neutralization assays, anti-mouse CD44 (BD Pharmingen) neutralizing antibody was used. CSPG-DS was added to PDL-cultured microglia at the indicated concentrations.

Assay of Nitric Oxide

Nitric oxide release was assayed according to the method of Griess [41].

RNA Purification, cDNA Synthesis, and Reverse Transcription PCR Analysis

These procedures were performed as previously described [18]. The following primers were used: tumor necrosis factor alpha (TNF-α), 5′-GGGACAGTGACCTGGACTGT-3′, 5′-

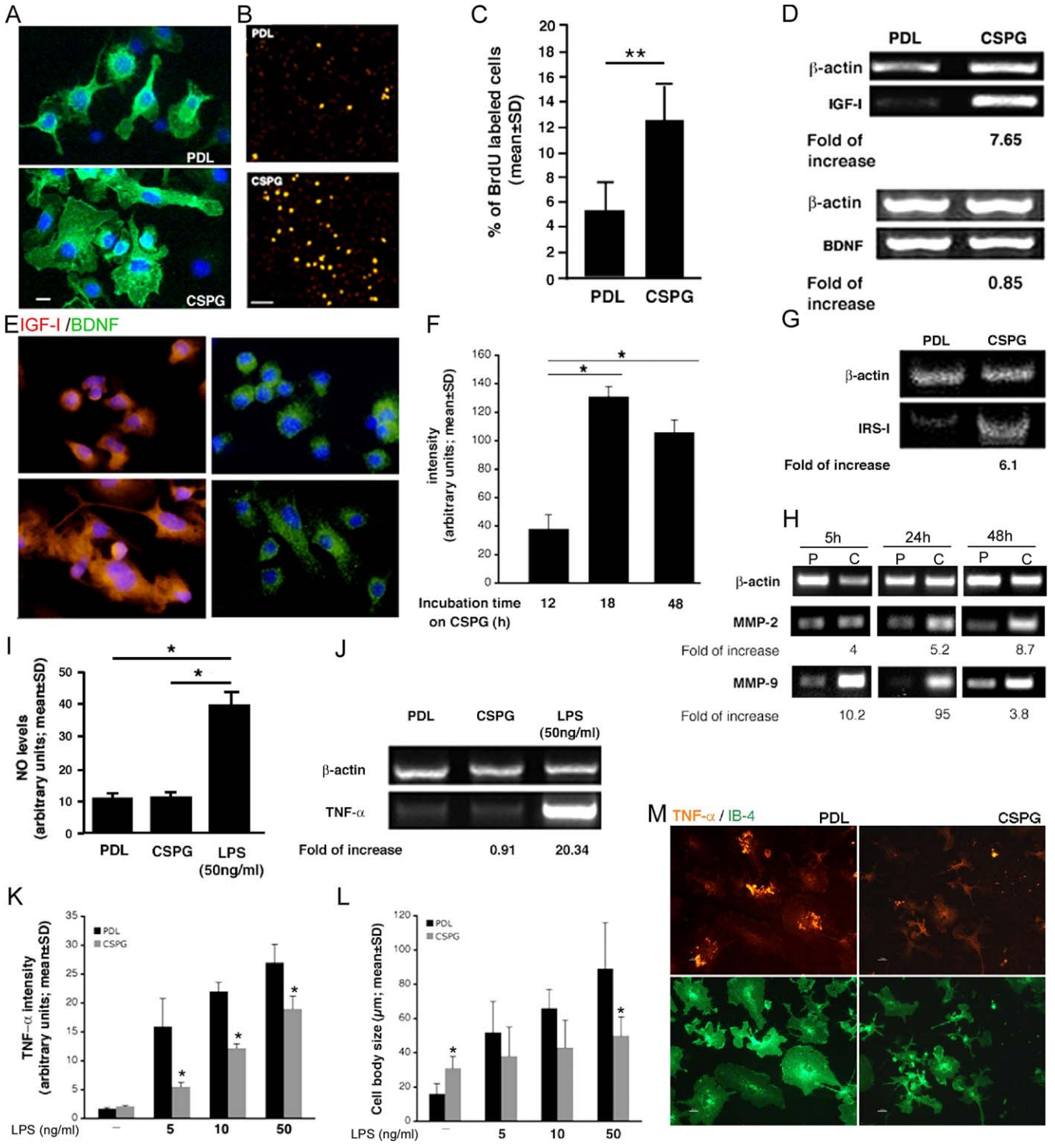

Figure 6. CSPG Activates Microglia to Acquire a Noncytotoxic, Beneficial Phenotype

(A) IB-4 labeling (green) and Hoechst (nuclear; blue) of microglia cultured on PDL or on CSPG for 48 h showing morphological changes in the CSPG-cultured microglia (scale bar, 10 μm).

(B) BrdU incorporation showing increased proliferation induced by microglia cultured on CSPG relative to PDL-cultured microglia (scale bar, 100 μm).

(C) Quantitative analysis of the proportion of BrdU-incorporating cells in the total population of IB-4+ cells (Student *t*-test, $t = 4.24$, $df = 6$, $p = 0.005$).

(D) Semi-quantitative PCR analyses of IGF-1 and BDNF expression by microglia cultured for 12 h on PDL or on CSPG. Values represent relative amounts of amplified mRNA normalized against β-actin in the same sample, and are represented as fold induction relative to control microglia cultured on PDL.

(E) IGF-1 (red) and BDNF (green) expression in microglia cultured for 18 h on PDL or on CSPG (scale bar, 20 μm). Hoechst labeling is blue.

(F) Quantitative analysis of IGF-1 immunoreactivity in microglia cultured for 12, 18, and 48 h on CSPG (ANOVA, $F[2,6] = 185.2$, $p = 0.0001$, followed by the Fisher test).

(G) Semi-quantitative PCR analyses of IRS-1 expression by microglia cultured on PDL and on CSPG.

(H) Semi-quantitative PCR analyses of MMP-2 and MMP-9 mRNA in microglia cultured on PDL and on CSPG for various time periods. Values represent relative amounts of amplified mRNA normalized against β-actin in the same sample, and are represented as fold change in microglia cultured on CSPG relative to PDL at the same time point (C, CSPG; P, PDL).

(I) Nitric oxide levels in the culture media of microglia cultured for 48 h on PDL or CSPG or in the presence of LPS (50 ng/ml) (ANOVA, $F[2,9] = 114.9$, $p = 0.0001$, followed by the Fisher test).
(J) Semi-quantitative PCR analysis of TNF-α expression indicating that TNF-α was not increased in CSPG-activated microglia, but was significantly increased upon activation of microglia by LPS (12 h). Values represent relative amounts of amplified mRNA normalized against β-actin in the same sample, and are represented as fold induction relative to control microglia cultured on PDL.
(K–M) Cells were cultured on PDL and CSPG, 24 h prior to their stimulation with LPS for an additional 24 h. Quantitative analysis of TNF-α production (K) or cell-body size (L) in microglia activated by increasing doses of LPS (M), representative photos; TNF-α (red) and IB-4 (green) labeling of microglia (scale bar, 20 μm). Two-way ANOVA was used for statistical analysis in (K) ($F[7,17] = 34.3$, $p = 0.0001$) and (L) ($F[7,53] = 19.47$, $p = 0.0001$), followed by the Fisher test ($^*p = 0.05$). The changes were significant between the CSPG- and PDL-cultured microglia. All data are from one of at least three independent experiments with replicate cultures. $^*p < 0.05$; $^{**}p < 0.01$.
doi:10.1371/journal.pmed.0050171.g006

AGGCTGTGCATTGCACCTCA-3′; insulin-like growth factor 1 (IGF-1), 5′-TGGATGCTCTTCAGTTCGTG-3′, 5′-GTCTTGGGCATGTCAGTGTG-3′; insulin receptor substrate 1 (IRS-1), 5′-AGCGAGCTCGAGCATGGCGAGCCCTC-3′, 5′-ATCGTCGACTCGAGATCTCCGAGTCA-3′; brain-derived neurotrophic factor (BDNF), 5′-GCTGACACTTTTGAGCAC-3′, 5′-AAATCCACTATCTTCCCC-3′; matrix metalloproteinase 2 (MMP-2), 5′-CTTCGCTCGTTTCCTTCAAC-3′, 5′-AGAGTGAGGAGGGGAACCAT-3′; MMP-9, 5′-TGAATCAGCTGGCTTTTGTG-3′, 5′GTGGATAGCTCGGTGGTGTT-3′; and β-actin, 5′-TAAAACGCAGCTCAGTAACAGTCCG-3′, 5′-TGGAATCCTGTGGCATCCATGAAAC-3′.

Statistical Analysis

Data were analyzed using the Student *t*-test to compare between two groups; two-way ANOVA followed by the Fisher LSD (least significant difference) procedure to compare between multiple numbers of groups and repeated ANOVA was used in the functional BMS scoring. The specific tests used to analyze each set of experiments are indicated in the legends.

Results

CSPG Present in the Lesion Site after Spinal Cord Injury Modulates Neurotrophic Factor Expression by Microglia/Macrophages

After CNS injury, microglia/macrophages become activated and accumulate at the lesion site. We first examined neurotrophic factor expression by these cells. We inflicted a well-calibrated contusive injury at the thoracic segments of the mice spinal cords (T-12), which resulted in paralysis of the hind limbs. To delineate the lesion site in spinal cord sections, we used GFAP labeling. We found that microglia/macrophages located at the lesion site expressed high levels of IGF-1 in addition to BDNF (Figure 1A and 1B, respectively). Quantitation of IGF-1 levels in tissue homogenates using ELISA revealed a 3-fold increase in a homogenate of tissue excised from the site of injury, relative to a homogenate of tissue excised from a region far from the injured site (mean ± SD: 175 ± 13.5 pg/ml in the lesion area compared to 55 ± 5.8 pg/ml in the distal area; $n = 4$). Immunohistochemical analysis revealed that IGF-1 was expressed mostly by the microglia/macrophages found at the margins of the lesion as opposed to BDNF, which was not specifically elevated in these cells (Figure 1C–1F).

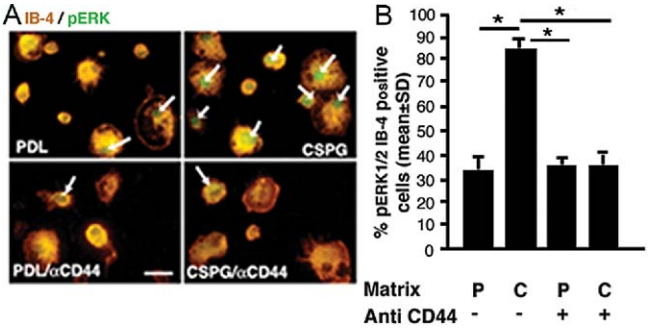

Figure 7. Microglial Activation by CSPG Is Mediated by CD44

(A) Anti-phospho-ERK1/2 labeling (green) indicating increased phosphorylation of ERK1/2 in microglia (IB-4; red) cultured on CSPG. In this culture, addition of CD44-neutralizing antibodies to the medium resulted in decreased ERK1/2 phosphorylation (scale bar, 20 μm). Arrows indicate microglia labeled with pERK1/2.
(B) Quantitative analysis of pERK1/2-positive, IB-4-positive cells. Data are from one of at least three independent experiments in replicate cultures (P, PDL; C, CSPG; ANOVA, $F[3,17] = 158.7$, $p = 0.0001$; followed by Fisher test, $^*p = 0.05$).
doi:10.1371/journal.pmed.0050171.g007

The observed localized expression of IGF-1 encouraged us to examine its association with CSPG, shown to be expressed mainly at the margins of the lesion. Immunohistochemical analysis showed that microglia/macrophages that were spatially associated with CSPG expressed IGF-1 in abundance (Figure 1D and 1E). In contrast, BDNF expression was not related to the presence of CSPG (Figure 1D and 1F).

The increased expression of IGF-1 by the microglia/macrophages that were spatially associated with CSPG could reflect a direct interaction of these cells with CSPG. Alternatively, it could be an outcome of additional differences between the margins and the epicenter of the lesion, such as the origin of the microglia/macrophages; a preferential presence of either microglia or blood-borne monocytes [42] at the margins of the lesion. To address this issue, we used chimeric mice whose bone marrow cells had been replaced in adulthood with green fluorescent protein (GFP)-expressing bone marrow cells (isolated from transgenic mice that express GFP in their myeloid cells [36]). First we determined the basal number of blood-borne monocytes (identified by their GFP expression) in naïve spinal cords of the chimeric mice. We did not detect any infiltrating blood-borne monocytes in the naïve cords (Figure 1G). A recent report identified approximately 3 ± 1 infiltrating cells per square millimeter, in a noninjured spinal cord under similar conditions [43]. Following injury, numerous infiltrating blood-borne monocytes (314 ± 185 cells/mm^2) were found at the margins of the lesion but almost none at the epicenter of the lesion (Figure 1G and 1H); nevertheless, a small number of GFP$^+$ (green) cells were also noted in the epicenter. Resident microglia, however, were distributed both in the margins and at the epicenter of the injured site (Figure 1I). Analysis of IGF-1 expression revealed that in the CSPG-rich areas both microglia and blood-borne monocytes expressed increased levels of IGF-1 (Figure 1J). These results strengthened our observation

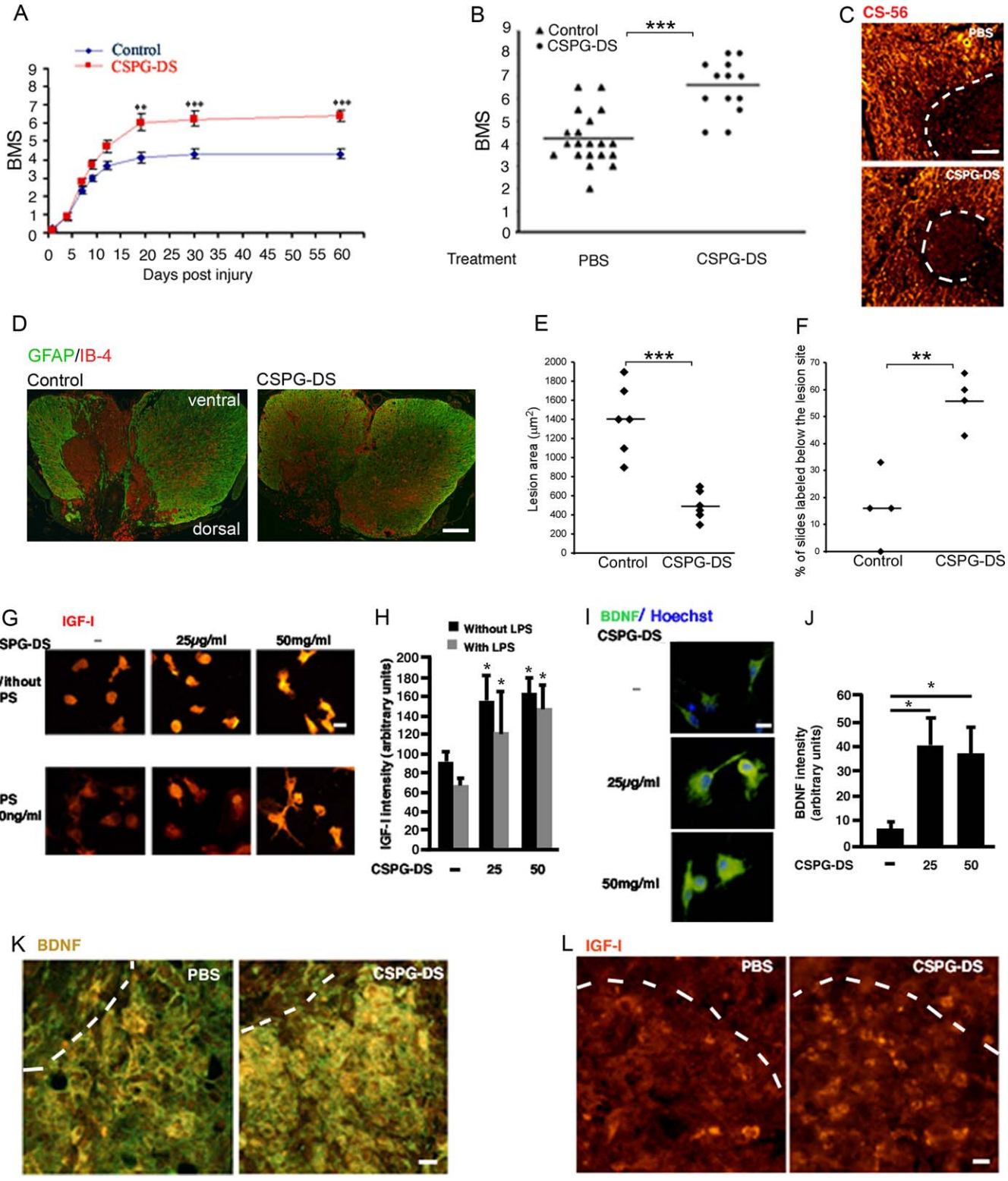

Figure 8. Systemic Administration of CSPG-DS Promotes Recovery after Spinal Cord Injury

(A) Mean locomotor score (BMS) for each group during the 60-d recovery period (repeated measures ANOVA, F[1,31] = 15.47 [between groups], $p = 0.0004$). After injuries of similar severity, recovery was significantly improved as a result of CSPG-DS treatment.

(B–D) BMS scores of individual mice on day 60 after spinal cord injury (Student *t*-test, $t = -5.52$, df = 31, $p = 0.0001$) (B). Spinal cord sections from injured mice treated with CSPG-DS (5 μg) or PBS were immunolabeled with CS-56 (CSPG, red; scale bar 100 μm) (C), GFAP (astrocytes, green), and IB-4 (microglia/macrophages, red; scale bar, 100 μm) of the lesion site in coronal sections (D).

(E) Quantitative analysis of the IB-4-labeled area, indicative of the lesion site (Student *t*-test, $t = -5.53$, df = 10, $p = 0.0003$).

(F) Quantitative analysis of BDA labeling. Sections that contained more than two labeled fibers caudal to the lesion site were counted and presented in percentage (Student *t*-test, $t = -4.81$, df = 6, $p = 0.003$).

(G) IGF-1 immunoreactivity (red) in microglia treated with CSPG-DS in the presence or absence of LPS (scale bar, 20 μm).

(H) Quantitative analysis of IGF-1 immunoreactivity in the CSPG-DS-treated microglia, with (gray) and without LPS (black) (ANOVA, $F[5,19] = 10.63$, $p = 0.0001$; followed by the Fisher test; the changes were significant at 95% between the CSPG-DS-treated microglia and the PBS-treated controls).
(I) BDNF immnoreactivity (green) and Hoechst labeling (blue) in microglia treated with CSPG-DS (scale bar, 10 μm).
(J) Quantitative analysis of BDNF immunoreactivity in the CSPG-DS-treated microglia (ANOVA, $F[2,9] = 23.16$, $p = 0.0003$; followed by the Fisher test).
(K) BDNF labeling (yellow) of microglia in the lesion site (scale bar, 20 μm). The image depicts the marginal area of the lesion.
(L) IGF-1 staining (red) of microglia in the lesion (scale 20 μm). The image depicts the epicenter of the lesion. The dashed line demarcates the lesion site.
All data in (G)–(J) are from one of at least three independent experiments with replicate cultures.
*$p < 0.05$; **$p < 0.01$; ***$p < 0.001$.
doi:10.1371/journal.pmed.0050171.g008

that expression of IGF-1 is determined by the location of the cells and their spatial association with the margin of the lesion.

CSPG Modulates Microglia/Macrophage Activation and Spatial Localization in the Lesion Site

To examine whether CSPG directly affects the microglia and the blood-borne monocytes found in its proximity, we used xyloside, a pharmacological inhibitor of CSPG biosynthesis. Xyloside inhibits the biosynthesis of CSPG, and has been previously used to study the role of CSPG in axonal growth both in vivo and in vitro [38,44]. We treated mice with xyloside immediately after injury. Using anti-CSPG antibody (CS-56), we verified that this treatment resulted in a decrease in CSPG accumulation (Figure 2A and 2B). We found that xyloside treatment significantly attenuated IGF-1 expression (Figure 2C and 2D). The reduction in IGF-1 expression was quantitatively verified by ELISA, using homogenate of tissues excised from the site of injury of PBS- and xyloside-treated mice (151 ± 23 pg/ml in the lesion area of PBS-treated compared to 93 ± 22 pg/ml in the xyloside-treated mice; mean ± SD obtained from eight animals, analyzed separately; $p < 0.001$; Student t-test). In line with the reported inverse relationship between IGF-1 and TNF-α levels [18,45], the xyloside treatment also caused an increase in TNF- levels (11 ± 1.29 pg/ml in the PBS-treated group compared to 16.9 ± 3.1 pg/ml in the xyloside treatment; $p = 0.004$ Student t-test) determined by ELISA. On the other hand, xyloside treatment had no effect on BDNF levels (Figure 2E and 2F). In the few areas within the margins where xyloside failed to fully inhibit CSPG formation, we detected IGF-1–expressing cells (Figure 2G). Xyloside treatment of spinally injured chimeric mice (with GFP-expressing blood-borne monocytes; Figure 2H) revealed that the disruption of CSPG deposition resulted in an infiltration of blood-borne macrophages into the epicenter of the lesion, an area where they were not found in the presence of CSPG (Figure 2I). The possibility that the changes in the infiltration of macrophages might reflect a change in blood or bone marrow composition caused by the xyloside treatment was excluded by the demonstration that the bone marrow architecture and cellular composition as well as the cell populations in the blood were not affected by xyloside treatment (Figure S1). Thus, our data indicate that the increased IGF-1 expression by microglia and blood-borne monocytes, and the spatial organization of these cells at the lesion site, are related to the presence of CSPG.

CSPG Plays a Key Role in Recovery from Spinal Cord Injury

To address the relevance of CSPG production to the recovery from injury, we first assessed the size of the lesion site by immunohistochemical analysis. Staining for myelin with Luxol fast blue, and for cell nuclei with Nissel, revealed a dose-dependent increase in the size of the lesion site in correlation with the increase in the xyloside dosages (Figure 3A and 3B). Labeling of astrocytes with GFAP and of microglia/macrophages with IB-4 yielded similar results with respect to the lesion size (Figure 3C), indicating that in the absence of CSPG, tissue damage is markedly increased.

To further evaluate the relevance of CSPG production to functional recovery, we performed an additional experiment applying xyloside immediately after injury, and assessed the functional recovery using the Basso Mouse Scale, BMS. This scale evaluates locomotion in an open field, where a score of 0 indicates complete paralysis and a score of 9 indicates normal function. Treatment with xyloside immediately after injury significantly reduced the spontaneous recovery, resulting in lower motor function of the hind limbs (Figure 3D). This result emphasizes that CSPG plays a beneficial role in the spontaneous recovery from spinal cord injury.

Distinct Effects of CSPG in the Acute and Subacute Phases after Spinal Cord Injury

The observed beneficial role of CSPG and the well-documented inhibitory effect of CSPG on axonal growth [1,9,10] raise an apparent discrepancy. We postulated that this discrepancy reflects a nonoptimal postinjury regulation of CSPG levels and timing. Thus, for example, although CSPG is needed to induce the neuroprotective phenotype of microglia/macrophages in the acute phase (from immediately after injury to 1 or 2 d later), its continuing production in the subsequent (subacute) phase might be overwhelming and thus inhibits axonal growth. To examine the possibility that timing is crucial factor in the presence of CSPG, we again employed the experimental paradigm of spinal cord injury, but this time applied xyloside at the subacute phase (2 d after injury) so that CSPG biosynthesis was restricted to the acute phase. As a control, we treated an additional group of spinally injured mice with xyloside on day 7 after injury, when CSPG levels are no longer increased, and therefore was not expected to be affected by xyloside treatment (Figure 4A). Application of xyloside 2 d after the insult (in the subacute phase) promoted motor functional recovery (Figure 4B and 4E), in contrast to its application immediately after the injury, when it was detrimental to recovery (Figure 4C and 4E). Application of xyloside at day 7 did not affect recovery (Figure 4D and 4E). Next, we examined whether these functional effects were also reflected by the extent of anterograde-labeled descending fibers, caudally to the lesion site, following the immediate (day 0) and delayed (day 2) treatment with xyloside. We subjected the mice to anterograde labeling by injecting the tracer BDA into their motor cortex. A higher percentage of BDA-labeled fibers could be seen caudally to the lesion site in the group that was treated with xyloside on day 2 after the injury compared to the group that was treated with xyloside immediately after injury (Figures 4F, 4G, and S2). Consistent with the functional and

morphological observations described above, the lesion site in the animals that received immediate xyloside treatment (day 0) was enlarged, while treatment delayed to day 2 resulted in a reduction in the size of the damaged site (Figure 4H and 4I) as detected by GFAP/IB-4 immunohistochemistry; treatment on day 7 had no functional or morphological effect. The different effects of xyloside treatment in the various regimes (day 0, 2, 7) further support the contention that the effect of xyloside is local on CSPG synthesis, rather than an unrelated systemic effect. Examining CSPG levels in the different treatment groups indicated that both in the immediate treatment (day 0) and in the delayed treatment (day 2), there was a decrease in the overall levels of CSPG detected by immunohistochemistry (Figure 4J and 4K) and by Western blotting (Figure 4L).

Based on these findings, we wished to examine whether the delayed (day 2) xyloside treatment, compared to the immediate treatment, differentially affected the microglia/macrophages and their distribution at the lesion site. We found that the inhibition of CSPG synthesis during the subacute phase (delayed [day 2] treatment), resulted in increased IGF-1 immunolabeling (Figure 5A) and increased protein secretion (determined by ELISA; Figure 5B) relative to the PBS control. Treatment on day 7 had no effect on IGF-1 levels. TNF-α levels, in contrast to those with the immediate inhibition of CSPG synthesis, were not affected by the delayed (day 2) treatment, while the immediate inhibition of CSPG synthesis resulted in increased TNF-α levels (11 ± 1.29 pg/ml in the PBS-treated group versus 16.9 ± 3.1 pg/ml in the xyloside treatment group; Student *t*-test, $p = 0.004$; $n = 4$ mice per group; determined by ELISA).

As described above, CSPG participated in the spatial organization of the microglia/macrophages at the lesion site; in the absence of CSPG (in mice receiving xyloside treatment immediately after the injury), the compartmentalized organization of the site was disrupted and macrophages also invaded the epicenter of the lesion (Figure 2I). We therefore analyzed the distribution of the blood-borne monocytes following delayed (day 2) treatment with xyloside, conditions that resulted in improved recovery. We found that when CSPG production was limited to the acute phase by the delayed administration of xyloside, the spatial organization of the microglia/macrophages at the lesion site was maintained (Figure 5C and 5D).

CSPG Activates Microglia to Acquire a Noncytotoxic, Beneficial Phenotype

To gain insight into the underlying mechanism of CSPG effects on microglia/macrophages, we employed in vitro assays using primary cultures of mouse microglia. Microglia cultured on an inert substrate, PDL, were used as a basal reference. Cultured microglia at rest do not show the classical ramified morphology of microglia in vivo [46]. Nevertheless, we observed morphological changes in the microglia cultured on CSPG relative to those cultured on PDL (Figure 6A). The morphology of microglia cultured on CSPG had a "fried egg" morphology, with flattened and thickened membrane processes and a larger cell body (mean ± SD 37 ± 10 μm in CSPG-cultured microglia versus 21 ± 5.6 μm on a PDL base; Student *t*-test, $p < 0.0001$), a morphology associated with microglial activation [47]. Increased incorporation of the cell-proliferation marker BrdU demonstrated significantly increased proliferation of the microglia cultured on CSPG relative to those cultured on PDL (Figure 6B and 6C).

Examination of the direct effect of CSPG on microglial expression of BDNF and IGF-1 in vitro, in line with our results in vivo, revealed an increase in the mRNA of IGF-1 but not of BDNF (Figure 6D). Analysis of the cells at the protein level revealed an increase in IGF-1 expression in microglia cultured on CSPG relative to those cultured on PDL (Figure 6E and 6F). However, no effect on the expression BDNF was observed (Figure 6E).

IGF-1 is recognized as a key factor in neuronal survival [48] and can act in either an autocrine or a paracrine manner [49,50]. Comparison of gene arrays of microglia cultured on CSPG versus those grown on PDL (Tables S1–S3) revealed that a group of IGF-1–related genes was increased after incubation of microglia on CSPG but not on PDL. In order to determine whether IGF-1 affects CSPG-activated microglia, and if the effect is autocrine in nature (as our gene array analysis suggested), we assayed the mRNA of IRS-1. Expression of IRS-1 is reportedly increased when microglia are activated by IGF-1 [51]. PCR analysis indeed revealed an increase in IRS-1 transcripts in the CSPG-activated microglia (Figure 6G).

MMPs are endogenous proteolytic enzymes that can degrade CSPG [52] and are reportedly expressed by activated microglia/macrophages [53,54]. Because of the relevance of these enzymes as potential players in the feedback regulation of CSPG levels in injured tissue, we examined the expression of MMP-2 and MMP-9, two of the most prominent MMPs in the injured CNS. mRNA levels of MMP-2 and MMP-9 were analyzed at different time points in microglia cultured on CSPG and compared to microglia cultured on PDL. Both MMP-2 and MMP-9 were more abundant in the CSPG-activated microglia than in the microglia cultured on PDL (Figure 6H). Compared to MMP-2, MMP-9 levels were increased at an earlier time point. Our data thus suggest that CSPG can directly activate microglia to express IGF-1 and MMPs.

Examination of the microglia cultured on CSPG revealed no detectable increase in nitric oxide (measured in terms of nitrate levels in the cultured media; Figure 6I) or in TNF-α mRNA (Figure 6J) relative to microglia cultured on PDL. In agreement with other studies, activation of microglia by LPS resulted in their expression of a cytotoxic phenotype [55] in which nitric oxide and TNF-α were markedly increased (Figure 6I and 6J). However, when we incubated microglia on CSPG before exposing them to LPS, their TNF-α production, determined by immunocytochemistry, was significantly lower than that produced by LPS-activated microglia that were not pre-exposed to CSPG (Figure 6K and 6M). In addition, the microglia cultured on CSPG, when subsequently exposed to LPS, differed from LPS-activated microglia with respect to the increase in cell-body size (Figure 6L and 6M). Taken together, our findings suggest that CSPG can balance out the production of potentially cytotoxic compounds and concomitantly induce expression of specific neurotrophic factors.

Interaction of Microglia with CSPG Is Mediated by the CD44 Receptor

CD44 is a well-characterized receptor of CSPG [55]. To determine whether the interaction of microglia with CSPG occurs, at least in part, via the CD44 receptor, we examined

the effect of CD44-neutralizing antibodies on downstream effector molecules. Activation by CD44 is known to induce phosphorylation of ERK1/2 [56]. Having first established immunocytochemically that ERK1/2 phosphorylation occurs in CSPG-activated microglia (Figure 7), we showed that such phosphorylation was significantly decreased by the addition of anti-CD44 neutralizing antibodies (Figure 7). CD44 activation has also been shown to induce expression of IGF-1 [57].

Products of CSPG Degradation Promote Recovery from Spinal Cord Injury

Some of the most important lines of evidence supporting a negative effect of CSPG on CNS repair come from studies in which degradation of CSPG by ChABC, even if it is administered immediately after an insult [1,12], results in improved recovery. Those results appear to contradict our present findings that when CSPG biosynthesis is prevented immediately after a spinal cord injury, recovery is worse than spontaneous recovery. This apparent discrepancy might be explained, at least in part, by the fact that degradation of molecules, unlike inhibition of biosynthesis, leads to the formation of new compounds that are themselves often functional [58]. Increasing evidence indicates that many degradation products of biological compounds themselves possess potent biological activity [58,59]. With respect to the proteoglycans, for example, sugar compounds derived from heparan sulfate proteoglycan were shown to participate in wound repair and termination of inflammatory responses [58,59].

In the case of CSPG, its degradation by ChABC results in the formation of a 6-sulfated disaccharide (CSPG-DS) [60], which exhibits potent neuroprotective properties in several models of neurotoxicity and neuronal degeneration [60]. Accordingly, we postulated that at least part of the reported beneficial effect of CSPG degradation might be attributable to this neuroprotective compound (and possibly also to others) formed as a result of its specific enzymatic degradation with ChABC. To examine the potential beneficial role of CSPG degradation products, we repeatedly injected CSPG-DS intravenously after spinal cord injury in mice. The choice of the dosage and the regimen (days 1, 4, 7, 10, and 13) was based on our previous study [60]. The mean BMS scores used to follow the functional recovery of groups of spinally injured mice treated with CSPG-DS or PBS are shown for each day tested (Figure 8A). Scores achieved by individual mice on day 60 are shown in Figure 8B. Mice treated with CSPG-DS recovered significantly better than PBS-treated controls, resulting in a degree of hind-limb coordination that was not observed in the PBS-treated group.

Immunohistochemical analysis of the lesion site using anti-CSPG antibody revealed that treatment with CSPG-DS had no effect on CSPG levels, indicating that the beneficial effect of CSPG-DS treatment was not caused indirectly by inhibition of CSPG expression (Figure 8C).

Staining for GFAP and IB-4 indicated significant tissue preservation in the CSPG-DS–treated mice relative to controls treated with PBS (Figure 8D and 8E), so to verify tissue preservation we analyzed the spinal cords of CSPG-DS treated or PBS-treated mice for the presence of descending fibers below the lesion site, using stereotactic anterograde tracing of BDA administered to the motor cortexes (Figure 8F).

We also examined the potential effects of CSPG-DS on microglia in vitro. Incubation of microglia on PDL in the presence of CSPG-DS resulted, as with the intact CSPG, in a dose-dependent increase in IGF-1 levels (Figure 8G and 8H). In contrast to the finding with intact CSPG, we also observed an increase in BDNF levels (Figure 8I and 8J). These results showed that intact CSPG and CSPG-DS do not have completely overlapping effects, indicating that they operate via different mechanisms of action. We also examined whether CSPG-DS can balance out the inhibitory effect of LPS on IGF-1 production. By preincubating microglia with CSPG-DS it was possible to overcome the LPS-induced inhibition of IGF-1 expression in vitro (Figure 8G and 8H).

To further study the effect of CSPG-DS in vivo, we examined the injured spinal cords treated with CSPG-DS or PBS for IGF-1 and BDNF (Figure 8K and 8L). Treatment with CSPG-DS significantly increased BDNF and IGF-1 in the injured site. The increase in IGF-1-expressing microglia was not restricted to the cells associated with the margins of the lesion (Figure 8L).

Discussion

The results of this study suggest that CSPG, an extracellular component of the glial scar, exerts a beneficial effect on CNS recovery from injury, in part by inducing IGF-1 and MMP expression by microglia/macrophages and attenuating TNF-α levels. This microglial modulation was mediated, at least in part, by the CD44 receptor. Our data further suggest that, following injury to the CNS, CSPG plays a beneficial role in its recovery that can be achieved only by careful regulation of its presence: blockage of CSPG production immediately after spinal cord injury decreased spontaneous recovery, whereas restriction of CSPG biosynthesis to the acute phase improved recovery.

The intensive secretion of CSPG reported after a CNS injury [1,10,42] has been largely blamed for the lack of axonal regeneration and the detrimental outcome following injuries to the spinal cord. Moreover, the increase in CSPG observed in various CNS pathologies (such as multiple sclerosis and Alzheimer disease) [61,62] led to the widespread perception that the postinjury production of CSPG is a manifestation of CNS malfunction. Accordingly, treatments were developed to overcome the growth-inhibitory effect of this molecule, mainly by inducing its degradation by the specific enzyme ChABC [12]. The results of the present study, however, highlight a novel aspect of this molecule in regulating the local immune response via modulation of microglia/macrophage expression of IGF-1 and suggest that the postinjury production of CSPG in the acute phase plays an important role in the repair process.

The contribution of blood-borne monocytes to the recovery is still a subject of debate [5,21,32,63–65]. Using chimeric mice with GFP-expressing blood-borne monocytes, we demonstrated that both microglia and macrophages that were found in CSPG-rich areas expressed IGF-1, a phenomenon that was abolished when CSPG production was inhibited. Thus the present study suggests that CSPG modulates the behavior of microglia/macrophages and thereby affects their contribution to the overall repair process.

Nevertheless, in vivo, it is likely that additional factors besides CSPG contribute to the behavior of resident and recruited cells. Moreover, CSPG itself might have additional differential effects on the activation of microglia or macrophages and regulate other aspects of microglial cell/macrophage phenotype (such as phagocytosis or neurotrophic factor secretion).

The direct role of CSPG in controlling microglial and macrophage behavior after spinal cord injury was demonstrated here by blockage of CSPG biosynthesis, rather than inducing its degradation of existing CSPG. Degradation, unlike blockage of biosynthesis, can result in the formation of potentially new CSPG-derived active compounds such as CSPG-DS. Blockage of biosynthesis immediately after the injury resulted in reduced expression of IGF-1 by microglia/macrophages, loss of cellular compartmentalization in the lesion site, and decreased functional recovery relative to untreated controls. In contrast, when CSPG biosynthesis was allowed to take place during the first 2 d and was then inhibited, this treatment resulted in enhanced recovery, preservation of the site organization and of neurotrophic factor levels. Moreover, since both treatments (immediate and delayed to day 2) resulted in overall decrease in CSPG levels, it is likely that the improved recovery observed in the delayed treatment (day 2) should be attributed mostly to the presence of CSPG in the acute phase after injury.

Thus, these results indicate that the effect of CSPG after spinal cord injury is not an all-or-none phenomenon; it is a function of timing and level. Accordingly, our observations might explain some of the results described in the literature, in which various conditions of enzymatic degradation led to differing extents of recovery. For example, moderate (rather than intense) application of CSPG-degrading enzymes was reportedly more effective than intensive degradation [66]. Other lines of evidence indicate that astrocytes (the main source of CSPG) are required in CNS repair [67,68], specifically in the acute phase after injury, but not in the chronic phase [67]. In agreement with our study, pharmacological blockage of the MMPs, a family of endogenous proteolytic enzymes that degrade CSPG in the glial scar [52], when limited to the first 3 d after spinal cord injury, improves locomotor activity [69]. Our study further suggests that in those studies in which a beneficial effect of CSPG degradation by ChABC was documented it was, at least in part, an outcome of the production of new molecules, for example disaccharides (CSPG-DS), rather than simply the elimination of CSPG. Accordingly, in the present study CSPG-DS did directly modulate the microglial phenotype both in vitro and in vivo, without affecting the levels of CSPG. Although we demonstrated that the intact CSPG and its disaccharidic derivatives can independently affect microglia and promote recovery, we did not rule out the possibility that glycosaminoglycans, the saccharidic component of the proteoglycan, are the relevant active components responsible for the beneficial activity of the intact CSPG.

The observation that CSPG induces MMP expression by microglia in vitro, in light of the need for temporally regulated degradation of CSPG in the process of repair, might point to a potential feedback regulation of CSPG by the same microglia/macrophages as those activated by it. This point, however, requires further investigation.

To conclude, our study does not argue against the beneficial effect of CSPG degradation, but rather suggests that the timing and the extent of degradation should be carefully selected according to the changing requirements of the ongoing dynamic repair process [70]. In its intact form, CSPG is required at the early stages of recovery to activate microglia/macrophages and possibly to limit the spread of damage by creating a physical barrier, whereas in the chronic postinjury phase, or when present in excessive amounts, CSPG inhibits axonal growth and regeneration. Regulation of CSPG expression may have a role in the repair of minor injuries but is inadequate for major CNS traumas. Moreover, since CSPG is a major constituent of the glial scar, the present findings raises the potential need to revisit the overall perception of the glial scar and its role in recovery. A better understanding of the regulation of the scar tissue and the role of the naturally occurring CSPG in health and disease will enable us to increase the benefit of endogenous repair mechanisms and improve many of the available therapies for CNS injury.

Supporting Information

Figure S1. Xyloside Application Following Spinal Cord Injury Does Not Affect Cellular Composition of the Blood or Bone Marrow

Found at doi:10.1371/journal.pmed.0050171.sg001 (1.9 MB TIF).

Figure S2. BDA Labeling Technique

Found at doi:10.1371/journal.pmed.0050171.sg002 (1 MB DOC).

Table S1. Genes Up-regulated on Microglia Cultured on CSPG Compared to PDL

Found at doi:10.1371/journal.pmed.0050171.st001 (238 KB XLS).

Table S2. Ease Score of Functional Groups of Up-regulated Genes in Microglia Cultured on CSPG Relative to PDL

Found at doi:10.1371/journal.pmed.0050171.st002 (63 KB XLS).

Table S3. Genes Down-regulated on Microglia Cultured on CSPG Compared to PDL

Found at doi:10.1371/journal.pmed.0050171.st003 (120 KB XLS).

Text S1. Supplementary Materials and Methods

Found at doi:10.1371/journal.pmed.0050171.sd001 (29 KB DOC).

Acknowledgments

We thank Dr. Stefan Jung for providing us with CX3CR1$^{GFP/+}$ mice, Hillary Voet for assistance with the statistical analysis, Shelley Schwarzbaum for editing the manuscript, and Yaniv Ziv, Gil Lewitus, Ayal Ronen, and Rinat Levi for their constructive comments. MS holds the Maurice and Ilse Katz Professorial Chair in Neuroimmunology.

Author contributions. AR and RS designed the experiments and carried them out with AL; AR, RS, and MS wrote the paper; YS helped with in vitro experiments. The gene array project was conducted by JJ-H, NA, and GR.

References

1. Silver J, Miller JH (2004) Regeneration beyond the glial scar. Nat Rev Neurosci 5: 146–156.
2. Buss A, Pech K, Kakulas BA, Martin D, Schoenen J, et al. (2007) Growth-modulating molecules are associated with invading Schwann cells and not astrocytes in human traumatic spinal cord injury. Brain 130: 940–953.
3. Fitch MT, Silver J (1997) Activated macrophages and the blood-brain barrier: inflammation after CNS injury leads to increases in putative inhibitory molecules. Exp Neurol 148: 587–603.
4. Fournier AE, Strittmatter SM (2001) Repulsive factors and axon regeneration in the CNS. Curr Opin Neurobiol 11: 89–94.
5. Popovich PG, Guan Z, Wei P, Huitinga I, van Rooijen N, et al. (1999) Depletion of hematogenous macrophages promotes partial hindlimb recovery and neuroanatomical repair after experimental spinal cord injury. Exp Neurol 158: 351–365.
6. Fleming JC, Norenberg MD, Ramsay DA, Dekaban GA, Marcillo AE, et al. (2006) The cellular inflammatory response in human spinal cords after injury. Brain 129: 3249–3269.
7. Stirling DP, Khodarahmi K, Liu J, McPhail LT, McBride CB, et al. (2004)

Minocycline treatment reduces delayed oligodendrocyte death, attenuates axonal dieback, and improves functional outcome after spinal cord injury. J Neurosci 24: 2182–2190.
8. Brambilla R, Bracchi-Ricard V, Hu WH, Frydel B, Bramwell A, et al. (2005) Inhibition of astroglial nuclear factor kappaB reduces inflammation and improves functional recovery after spinal cord injury. J Exp Med 202: 145–156.
9. Properzi F, Asher RA, Fawcett JW (2003) Chondroitin sulphate proteoglycans in the central nervous system: changes and synthesis after injury. Biochem Soc Trans 31: 335–336.
10. Matsui F, Oohira A (2004) Proteoglycans and injury of the central nervous system. Congenit Anom (Kyoto) 44: 181–188.
11. Jones LL, Yamaguchi Y, Stallcup WB, Tuszynski MH (2002) NG2 is a major chondroitin sulfate proteoglycan produced after spinal cord injury and is expressed by macrophages and oligodendrocyte progenitors. J Neurosci 22: 2792–2803.
12. Bradbury EJ, Moon LD, Popat RJ, King VR, Bennett GS, et al. (2002) Chondroitinase ABC promotes functional recovery after spinal cord injury. Nature 416: 636–640.
13. McKerracher L (2001) Spinal cord repair: strategies to promote axon regeneration. Neurobiol Dis 8: 11–18.
14. Moalem G, Leibowitz-Amit R, Yoles E, Mor F, Cohen IR, et al. (1999) Autoimmune T cells protect neurons from secondary degeneration after central nervous system axotomy. Nat Med 5: 49–55.
15. Bechmann I, Nitsch R (2001) Plasticity following lesion: help and harm from the immune system. Restor Neurol Neurosci 19: 189–198.
16. Hofstetter HH, Sewell DL, Liu F, Sandor M, Forsthuber T, et al. (2003) Autoreactive T cells promote post-traumatic healing in the central nervous system. J Neuroimmunol 134: 25–34.
17. Simard AR, Rivest S (2006) Neuroprotective properties of the innate immune system and bone marrow stem cells in Alzheimer's disease. Mol Psychiatry 11: 327–335.
18. Butovsky O, Ziv Y, Schwartz A, Landa G, Talpalar AE, et al. (2006) Microglia activated by IL-4 or IFN-gamma differentially induce neurogenesis and oligodendrogenesis from adult stem/progenitor cells. Mol Cell Neurosci 31: 149–160.
19. Qin H, Wilson CA, Lee SJ, Zhao X, Benveniste EN (2005) LPS induces CD40 gene expression through the activation of NF-kappaB and STAT-1alpha in macrophages and microglia. Blood 106: 3114–3122.
20. van Rossum D, Hanisch UK (2004) Microglia. Metab Brain Dis 19: 393–411.
21. Yin Y, Cui Q, Li Y, Irwin N, Fischer D, et al. (2003) Macrophage-derived factors stimulate optic nerve regeneration. J Neurosci 23: 2284–2293.
22. Seguin R, Biernacki K, Prat A, Wosik K, Kim HJ, et al. (2003) Differential effects of Th1 and Th2 lymphocyte supernatants on human microglia. Glia 42: 36–45.
23. Beers DR, Henkel JS, Xiao Q, Zhao W, Wang J, et al. (2006) Wild-type microglia extend survival in PU.1 knockout mice with familial amyotrophic lateral sclerosis. Proc Natl Acad Sci U S A 103: 16021–16026.
24. Li L, Lu J, Tay SS, Moochhala SM, He BP (2007) The function of microglia, either neuroprotection or neurotoxicity, is determined by the equilibrium among factors released from activated microglia in vitro. Brain Res 1159: 8–17.
25. Meda L, Cassatella MA, Szendrei GI, Otvos L Jr., Baron P, et al. (1995) Activation of microglial cells by beta-amyloid protein and interferon-gamma. Nature 374: 647–650.
26. Minagar A, Shapshak P, Fujimura R, Ownby R, Heyes M, et al. (2002) The role of macrophage/microglia and astrocytes in the pathogenesis of three neurologic disorders: HIV-associated dementia, Alzheimer disease, and multiple sclerosis. J Neurol Sci 202: 13–23.
27. Majed HH, Chandran S, Niclou SP, Nicholas RS, Wilkins A, et al. (2006) A novel role for Sema3A in neuroprotection from injury mediated by activated microglia. J Neurosci 26: 1730–1738.
28. Nagele RG, Wegiel J, Venkataraman V, Imaki H, Wang KC (2004) Contribution of glial cells to the development of amyloid plaques in Alzheimer's disease. Neurobiol Aging 25: 663–674.
29. Blasko I, Stampfer-Kountchev M, Robatscher P, Veerhuis R, Eikelenboom P, et al. (2004) How chronic inflammation can affect the brain and support the development of Alzheimer's disease in old age: the role of microglia and astrocytes. Aging Cell 3: 169–176.
30. Ghasemlou N, Jeong SY, Lacroix S, David S (2007) T cells contribute to lysophosphatidylcholine-induced macrophage activation and demyelination in the CNS. Glia 55: 294–302.
31. Block ML, Zecca L, Hong JS (2007) Microglia-mediated neurotoxicity: uncovering the molecular mechanisms. Nat Rev Neurosci 8: 57–69.
32. Glezer I, Simard AR, Rivest S (2007) Neuroprotective role of the innate immune system by microglia. Neuroscience 147: 867–883.
33. Neumann J, Gunzer M, Gutzeit HO, Ullrich O, Reymann KG, et al. (2006) Microglia provide neuroprotection after ischemia. FASEB J 20: 714–716.
34. Streit WJ (2005) Microglia and neuroprotection: implications for Alzheimer's disease. Brain Res Brain Res Rev 48: 234–239.
35. Zou XH, Foong WC, Cao T, Bay BH, Ouyang HW, et al. (2004) Chondroitin sulfate in palatal wound healing. J Dent Res 83: 880–885.
36. Jung S, Aliberti J, Graemmel P, Sunshine MJ, Kreutzberg GW, et al. (2000) Analysis of fractalkine receptor CX(3)CR1 function by targeted deletion and green fluorescent protein reporter gene insertion. Mol Cell Biol 20: 4106–4114.
37. Basso DM, Fisher LC, Anderson AJ, Jakeman LB, McTigue DM, et al. (2006) Basso Mouse Scale for locomotion detects differences in recovery after spinal cord injury in five common mouse strains. J Neurotrauma 23: 635–659.
38. Zuo J, Hernandez YJ, Muir D (1998) Chondroitin sulfate proteoglycan with neurite-inhibiting activity is up-regulated following peripheral nerve injury. J Neurobiol 34: 41–54.
39. Herzog A, Brosamle C (1997) 'Semifree-floating' treatment: a simple and fast method to process consecutive sections for immunohistochemistry and neuronal tracing. J Neurosci Methods 72: 57–63.
40. Shechter R, Ziv Y, Schwartz M (2007) New GABAergic interneurons supported by myelin-specific T cells are formed in intact adult spinal cord. Stem Cells 25: 2277–2282.
41. Green LC, Wagner DA, Glogowski J, Skipper PL, Wishnok JS, et al. (1982) Analysis of nitrate, nitrite, and [15N]nitrate in biological fluids. Anal Biochem 126: 131–138.
42. Popovich PG, Hickey WF (2001) Bone marrow chimeric rats reveal the unique distribution of resident and recruited macrophages in the contused rat spinal cord. J Neuropathol Exp Neurol 60: 676–685.
43. Mildner A, Schmidt H, Nitsche M, Merkler D, Hanisch UK, et al. (2007) Microglia in the adult brain arise from Ly-6ChiCCR2+ monocytes only under defined host conditions. Nat Neurosci 10: 1544–1553.
44. Mendes FA, Onofre GR, Silva LC, Cavalcante LA, Garcia-Abreu J (2003) Concentration-dependent actions of glial chondroitin sulfate on the neuritic growth of midbrain neurons. Brain Res Dev Brain Res 142: 111–119.
45. Zhao W, Xie W, Xiao Q, Beers DR, Appel SH (2006) Protective effects of an anti-inflammatory cytokine, interleukin-4, on motoneuron toxicity induced by activated microglia. J Neurochem 99: 1176–1187.
46. Kettenmann H (2006) Triggering the brain's pathology sensor. Nat Neurosci 9: 1463–1464.
47. Soltys Z, Ziaja M, Pawlinski R, Setkowicz Z, Janeczko K (2001) Morphology of reactive microglia in the injured cerebral cortex. Fractal analysis and complementary quantitative methods. J Neurosci Res 63: 90–97.
48. Carro E, Trejo JL, Nunez A, Torres-Aleman I (2003) Brain repair and neuroprotection by serum insulin-like growth factor I. Mol Neurobiol 27: 153–162.
49. O'Donnell SL, Frederick TJ, Krady JK, Vannucci SJ, Wood TL (2002) IGF-I and microglia/macrophage proliferation in the ischemic mouse brain. Glia 39: 85–97.
50. Walter HJ, Berry M, Hill DJ, Logan A (1997) Spatial and temporal changes in the insulin-like growth factor (IGF) axis indicate autocrine/paracrine actions of IGF-I within wounds of the rat brain. Endocrinology 138: 3024–3034.
51. Tamemoto H, Kadowaki T, Tobe K, Yagi T, Sakura H, et al. (1994) Insulin resistance and growth retardation in mice lacking insulin receptor substrate-1. Nature 372: 182–186.
52. Hsu JY, McKeon R, Goussev S, Werb Z, Lee JU, et al. (2006) Matrix metalloproteinase-2 facilitates wound healing events that promote functional recovery after spinal cord injury. J Neurosci 26: 9841–9850.
53. Rosenberg GA, Cunningham LA, Wallace J, Alexander S, Estrada EY, et al. (2001) Immunohistochemistry of matrix metalloproteinases in reperfusion injury to rat brain: activation of MMP-9 linked to stromelysin-1 and microglia in cell cultures. Brain Res 893: 104–112.
54. Ihara M, Tomimoto H, Kinoshita M, Oh J, Noda M, et al. (2001) Chronic cerebral hypoperfusion induces MMP-2 but not MMP-9 expression in the microglia and vascular endothelium of white matter. J Cereb Blood Flow Metab 21: 828–834.
55. Bi XL, Yang JY, Dong YX, Wang JM, Cui YH, et al. (2005) Resveratrol inhibits nitric oxide and TNF-alpha production by lipopolysaccharide-activated microglia. Int Immunopharmacol 5: 185–193.
56. Bourguignon LY, Gilad E, Rothman K, Peyrollier K (2005) Hyaluronan-CD44 interaction with IQGAP1 promotes Cdc42 and ERK signaling, leading to actin binding, Elk-1/estrogen receptor transcriptional activation, and ovarian cancer progression. J Biol Chem 280: 11961–11972.
57. Noble PW, Lake FR, Henson PM, Riches DW (1993) Hyaluronate activation of CD44 induces insulin-like growth factor-1 expression by a tumor necrosis factor-alpha-dependent mechanism in murine macrophages. J Clin Invest 91: 2368–2377.
58. Ekre HP, Naparstek Y, Lider O, Hyden P, Hagermark O, et al. (1992) Anti-inflammatory effects of heparin and its derivatives: inhibition of complement and of lymphocyte migration. Adv Exp Med Biol 313: 329–340.
59. Ariel A, Yavin EJ, Hershkoviz R, Avron A, Franitza S, et al. (1998) IL-2 induces T cell adherence to extracellular matrix: inhibition of adherence and migration by IL-2 peptides generated by leukocyte elastase. J Immunol 161: 2465–2472.
60. Rolls A, Avidan H, Cahalon L, Schori H, Bakalash S, et al. (2004) A disaccharide derived from chondroitin sulphate proteoglycan promotes central nervous system repair in rats and mice. Eur J Neurosci 20: 1973–1983.
61. DeWitt DA, Silver J (1996) Regenerative failure: a potential mechanism for neuritic dystrophy in Alzheimer's disease. Exp Neurol 142: 103–110.
62. Sobel RA, Ahmed AS (2001) White matter extracellular matrix chondroitin

sulfate/dermatan sulfate proteoglycans in multiple sclerosis. J Neuropathol Exp Neurol 60: 1198–1207.
63. Rapalino O, Lazarov-Spiegler O, Agranov E, Velan GJ, Yoles E, et al. (1998) Implantation of stimulated homologous macrophages results in partial recovery of paraplegic rats. Nat Med 4: 814–821.
64. Turrin NP, Rivest S (2006) Molecular and cellular immune mediators of neuroprotection. Mol Neurobiol 34: 221–242.
65. David S, Bouchard C, Tsatas O, Giftochristos N (1990) Macrophages can modify the nonpermissive nature of the adult mammalian central nervous system. Neuron 5: 463–469.
66. Tom VG, Colman C, Shumsky JS, Houle JD (2006) Digestion of chondroitin sulfate proteoglycans with high concentrations of chondroitinase ABC after spinal cord injury augments tissue damage and increases functional deficits. Atlanta (Georgia): Neuroscience Meeting Planner. Society for Neuroscience. Abstract 383.18/NN71. Available: http://www.sfn.org/index.cfm?pagename=abstracts__ampublications. Accessed 14 July 2008.
67. Okada S, Nakamura M, Katoh H, Miyao T, Shimazaki T, et al. (2006) Conditional ablation of Stat3 or Socs3 discloses a dual role for reactive astrocytes after spinal cord injury. Nat Med 12: 829–834.
68. Faulkner JR, Herrmann JE, Woo MJ, Tansey KE, Doan NB, et al. (2004) Reactive astrocytes protect tissue and preserve function after spinal cord injury. J Neurosci 24: 2143–2155.
69. Noble LJ, Donovan F, Igarashi T, Goussev S, Werb Z (2002) Matrix metalloproteinases limit functional recovery after spinal cord injury by modulation of early vascular events. J Neurosci 22: 7526–7535.
70. Bareyre FM, Schwab ME (2003) Inflammation, degeneration and regeneration in the injured spinal cord: insights from DNA microarrays. Trends Neurosci 26: 555–563.

Editors' Summary

Background. Every year, spinal cord injuries paralyze about 10,000 people in the United States. The spinal cord, which contains bundles of nervous system cells called neurons, is the communication superhighway between the brain and the body. Messages from the brain travel down the spinal cord to control movement, breathing, and other bodily functions; messages from the skin and other sensory organs travel up the spinal cord to keep the brain informed about the body. All these messages are transmitted along axons, long extensions on the neurons. The spinal cord is protected by the bones of the spine but if these are displaced or broken, the axons can be compressed or cut, which interrupts the information flow. Damage near the top of the spinal cord paralyzes the arms and legs (tetraplegia); damage lower down paralyzes the legs only (paraplegia). Spinal cord injuries also cause other medical problems, including the loss of bowel and bladder control. Currently there is no effective treatment for spinal cord injuries. Treatment with drugs to reduce inflammation has, at best, only modest effects. Moreover, because damaged axons rarely regrow, most spinal cord injuries are permanent.

Why Was This Study Done? One barrier to recovery after a spinal cord injury seems to be an inappropriate immune response to the injury. After an injury, microglia (immune system cells that live in the nervous system), and macrophages (blood-borne immune system cells that infiltrate the injury) become activated. Microglia/macrophage activation can be either beneficial (the cells make IGF-1, a protein that stimulates axon growth) or destructive (the cells make TNF-α, a protein that kills neurons), so studies of microglia/macrophage activation might suggest ways to treat spinal cord injuries. Another possible barrier to recovery is "chondroitin sulfate proteoglycan" (CSPG). This is a major component of the scar tissue (the "glial scar") that forms around spinal cord injuries. CSPG limits axon regrowth, so attempts have been made to improve spinal cord repair by removing CSPG. But if CSPG prevents spinal cord repair, why is so much of it made immediately after an injury? In this study, the researchers investigate this paradox by asking whether CSPG made in the right place and in the right amount might have a beneficial role in spinal cord repair that has been overlooked.

What Did the Researchers Do and Find? The researchers bruised a small section of the spinal cord of mice to cause hind limb paralysis, and then monitored the recovery of movement in these animals. They also examined the injured tissue microscopically, looked for microglia and infiltrating macrophages at the injury site, and measured the production of IGF-1 and TNF-α by these cells. Inhibition of CSPG synthesis immediately after injury impaired the functional recovery of the mice and increased tissue loss at the injury site. It also altered the spatial organization of infiltrating macrophages at the injury site, reduced IGF-1 production by these microglia/macrophages, and increased TNF-α levels. In contrast, when CSPG synthesis was not inhibited until two days after the injury, the mice recovered well from spinal cord injury. Furthermore, the interaction of CSPG with a cell-surface protein called CD44 activated microglia/macrophages growing in dishes and increased their production of IGF-1 but not of molecules that kill neurons.

What Do These Findings Mean? These findings suggest that, immediately after a spinal cord injury, CSPG is needed for the repair of injured neurons and the recovery of movement, but that later on the presence of CSPG hinders repair. The findings also indicate that CSPG has these effects, at least in part, because it regulates the activity and localization of microglia and macrophages at the injury site and thus modulates local immune responses to the damage. Results obtained from experiments done in animals do not always accurately reflect the situation in people, so these findings need to be confirmed in patients with spinal cord injuries. However, they suggest that the effect of CSPG on spinal cord repair is not an inappropriate response to the injury, as is widely believed. Consequently, careful manipulation of CSPG levels might improve outcomes for people with spinal cord injuries.

Additional Information. Please access these Web sites via the online version of this summary at http://dx.doi.org/10.1371/journal.pmed.0050171.

- The MedlinePlus encyclopedia provides information about spinal cord injuries; MedlinePlus provides an interactive tutorial and a list of links to additional information about spinal cord injuries (in English and Spanish)
- The US National Institute of Neurological Disorders and Stroke also provides information about spinal cord injury (in English and Spanish)
- Wikipedia has a page on glial scars (note: Wikipedia is a free online encyclopedia that anyone can edit; available in several languages)